Trends in Hydrology, 1 (1994)

Hydrological impacts of climate change on the Laurentian Great Lakes[1]

Thomas E. Croley II
Great Lakes Environmental Research Laboratory, National Oceanic and Atmospheric Administration, 2205 Commonwealth Blvd., Ann Arbor, Michigan 48105-1593, USA

ABSTRACT

The Great Lakes Environmental Research Laboratory (GLERL) used their conceptual models for simulating moisture storages in, and runoff from, the 121 watersheds draining into the Laurentian Great Lakes, over-lake precipitation into each lake, and the heat storages in, and evaporation from, each lake. GLERL combined these components as net water supplies for each lake to consider climate change scenarios, developed from general circulation models of the global atmosphere, through linkages on air temperature, precipitation, humidity, wind speed, and cloud cover. Steady-state doubling of atmospheric CO_2 was considered by abstracting changes in linkages, making these changes in historical data, observing the impact of the changed data in the model outputs, and comparing it to model results using unchanged data, representing comparison to an unchanged atmosphere. This study indicates a 20 to 100% reduction in net basin supplies for each of the Great Lakes. The basins' various moisture storages become dryer and the lakes are warmer with associated hydrological impacts.

APPENDIX - NOTATION

a = wind parameter, T > 3.98°C ***[evaporation model empirical parameter]***
a' = wind parameter, T < 3.98°C ***[evaporation model empirical parameter]***
a_s = proportionality constant for snowmelt per degree-day ***[runoff model empirical parameter]***
A = area of the ice surface
A_b = area of the watershed
A_w = area of the open-water (ice-free) lake surface
α_{dp} = deep percolation coefficient ***[runoff model empirical parameter]***
α_{gw} = groundwater coefficient ***[runoff model empirical parameter]***
α_{int} = interflow coefficient ***[runoff model empirical parameter]***
α_{per} = percolation coefficient ***[runoff model empirical parameter]***
α_{sf} = surface outflow coefficient ***[runoff model empirical parameter]***
b = wind parameter, T > 3.98°C ***[evaporation model empirical parameter]***
b' = wind parameter, T < 3.98°C ***[evaporation model empirical parameter]***
b_1 = empirical constant
b_2 = empirical constant
β = partial linear reservoir coefficient
β_{eg} = groundwater zone evapotranspiration coefficient ***[runoff model empirical parameter]*** (= 0)
β_{el} = lower zone evapotranspiration coefficient ***[runoff model empirical parameter]*** (= 0)
β_{es} = surface zone evapotranspiration coefficient ***[runoff model empirical parameter]***
β_{eu} = upper zone evapotranspiration coefficient ***[runoff model empirical parameter]***
C_i = specific heat of ice
C_p = specific heat of air at constant temperature
C_w = specific heat of water
C_E = bulk evaporation coefficient over water
C'_E = bulk evaporation coefficient over ice
C_H = sensible heat coefficient over water
C'_H = sensible heat coefficient over ice
D = ice pack depth (thickness)
DD = degree-days per day
Δ = time increment of mass balance computation period
e = evaporation or evapotranspiration rate
e_p = rate of evaporation or evapotranspiration still possible
e_w = over-water evaporation rate
e'_w = over-ice evaporation rate
E = volumetric rate of evaporation from ice
E_g = evapotranspiration from the groundwater

[1]GLERL Contribution No. 876

zone storage

E_l = evapotranspiration from the lower soil zone storage

E_s = evapotranspiration from the surface storage

E_u = evapotranspiration from the upper soil zone storage

ε_w = emissivity of water

ε_a = emissivity of the atmosphere

f = infiltration rate

$f_{k,m}$ = ratio of surface temperature rise on day k from heat added on day m to that heat addition

F = representing lake volume at which a heat addition is uniformly fully mixed, T > 3.98°C ***[evaporation model empirical parameter]***

F' = representing lake volume at which a heat addition is uniformly fully mixed, T < 3.98°C ***[evaporation model empirical parameter]***

GZM = content of groundwater zone

γ_f = latent heat of fusion

γ_v = latent heat of vaporization

H = heat stored in the lake

H' = heat stored in the ice pack

H_s = nonlatent heat released to the atmosphere

η = parameter relating cloudiness to atmospheric longwave radiation ***[evaporation model empirical parameter]***

K = units and proportionality constant

LSZM = moisture content of lower soil zone

m = daily snowmelt rate

m_p = daily potential snowmelt rate

$M_{k,m}$ = mixing volume size on day k of heat added on day m

n = number of days in the mass balance computation period

ns = daily net supply rate to the watershed surface

N = fraction of sky covered in clouds

p = precipitation rate

q = specific humidity of the air over the water

q' = specific humidity of the air over the ice

q_0 = unit (per unit area) cloudless sky short-wave radiation rate

q_e = unit evaporative (latent and advected) heat transfer rate

q_e' = unit evaporative (latent and advected) heat transfer rate from ice pack

q_h = unit sensible heat transfer rate

q_h' = unit sensible heat transfer rate to ice pack

q_i = unit incident shortwave radiation rate

q_p = unit precipitation heat advection rate to water surface

q_p' = unit precipitation heat advection rate to ice pack

q_r = unit reflected shortwave radiation rate

q_r' = unit reflected shortwave radiation rate to ice pack

q_w = specific humidity of saturated air at temperature of water

q_w' = specific humidity of saturated air at temperature of ice

$q_\uparrow$ = longwave radiation emitted by the water body

$q_\downarrow$ = longwave radiation from the atmosphere absorbed by the water surface

Q = basin outflow volume for n days

Q_a = heat flux between atmosphere and ice pack used for freezing or melting

Q_l = net longwave radiation exchange rate

Q_w = total heat flux between the water body and the ice pack

Q_I = net heat advection to the lake from surface flows

Θ_i = sum of all surface inflows to lake

Θ_o = sum of all outflows from lake

r_a = reflectivity of the water surface

rr = daily solar insolation at the watershed surface

ρ = density of ice

ρ_a = density of air

ρ_w = density of water

S = volumetric rate of snow falling on ice

SNW = water content of the snowpack

SS = content of surface storage zone

σ = Stephan-Bolzman constant

t = time

T = water surface temperature

T' = ice surface temperature

T_a = air temperature

T_a' = over-ice air temperature

T_b = a base scaling temperature ***[runoff model empirical parameter]***

T_{max} = maximum daily air temperature

T_{min} = minimum daily air temperature

τ = daily extra-terrestrial solar radiation

τ_a = parameter reflecting ice pack shape, vertical-lateral change ratios along atmosphere-ice boundary, and ice buoyancy ***[evaporation model empirical parameter]***

τ_w = parameter reflecting ice pack shape, vertical-lateral change ratios along water-ice boundary, and ice buoyancy ***[evaporation model empirical parameter]***

U = wind speed over water

USZC = capacity of the upper soil zone (= 2 cm)

USZM = moisture content of upper soil zone

V = volume of the ice pack

V' = volume of ice formed by only by freezing or melting

V_c = lake volume (capacity)

V_e = equilibrium lake volume approached as a limit by mixing ***[evaporation model empirical parameter]***

W = daily wind movement

X = ratio of hours of bright sunshine to maximum possible
Ψ = total heat available for evapotranspiration during the day
Z = volume of water in storage

INTRODUCTION

Climatic change will impact on many aspects of the hydrologic cycle with consequences for mankind that are interrelated and often-times difficult to discern. A doubling of atmospheric CO_2 will have impacts on Great Lakes water supply components and basin storages of water and heat that must be understood before lake level impacts can be assessed. Because the Laurentian Great Lakes possess tremendous water and heat storage capacities, they respond slowly to changed meteorologic inputs. This "memory" results in a filtering or dampening of most short-term meteorologic fluctuations and in a response to longer-period fluctuations characteristic of climate change. Thus the large Great Lakes system is ideal for studying regional effects of climate changes.

Preliminary estimates of the impact of climatic warming on the Great Lakes water resources have been undertaken and are summarized elsewhere (Croley and Hartmann, 1989; Croley, 1990). The Environmental Protection Agency (EPA) coordinated several regional studies of various impacts of a doubling of atmospheric CO_2 at the direction of the U.S. Congress. As part of that study, the Great Lakes Environmental Research Laboratory (GLERL) assessed steady-state and transient changes in Great Lakes hydrology consequent with simulated atmospheric scenarios from three general circulation models (GCMs). Those studies, in part, and the high water levels of the late 1980s prompted the International Joint Commission to reassess climate change impacts on Great Lakes hydrology and lake thermal structure.

The methodology established in the EPA studies was adopted with slight modifications for use in the IJC studies. The methodology integrates hydrology and lake heat storage models (Croley, 1991, 1992b) to consider climate scenarios supplied by the Canadian Climate Centre (CCC) from its GCM (Louie, 1991; McFarlane, 1991). Cohen (1991) discusses the problems with this approach. The CCC provided a "present-climate" meteorology simulation ($1xCO_2$) and a changed-climate scenario ($2xCO_2$) developed from their atmospheric global circulation model. GLERL abstracted differences between the CCC-generated $1xCO_2$ and $2xCO_2$ atmospheres, made these changes to historical data, and observed the impact of the changed data in the hydrological outputs of their models.

The EPA studies included partial assessments of large-lake heat storage associated with climate change on Lakes Michigan (McCormick, 1989) and Erie (Blumberg and DiToro, 1989). The IJC study looked in less detail but more breadth at large-lake thermodynamics in that while only lake-wide effects were considered, all lakes were assessed. This paper briefly describes the Great Lakes, outlines GLERL's hydrological models and their applicability, presents the methodology of linkage between regional hydrological models and the GCMs as used especially in the IJC studies, describes their limitations, and presents and interprets the IJC studies of hydrological changes predicted through use of the Canadian Climate Centre's GCM.

GREAT LAKES SYSTEM

The Laurentian Great Lakes contain 23,000 km^3 of water (about 20% of the world's fresh surface water) and, with their surrounding basins, cover 770,000 km^2 in the United States and Canada; see Fig. 1. The lakes' surface areas comprise about one-third of the total basin area. The basin extends over 3200 km from the western edge of Lake Superior to the Moses-Saunders Power Dam on the St. Lawrence River. The water surface drops in a cascade over this distance more than 182 meters to sea level. The most upstream, largest, and deepest lake, is Lake Superior. The lake has two interbasin diversions of water into the system from the Hudson Bay basin, the Ogoki and Long Lac diversions. Lake Superior waters flow through the lock and compensating works at Sault Ste. Marie, Michigan and down the St. Marys River into Lake Huron where it is joined by water flowing from Lake Michigan through the Straits of Mackinac.

Another interbasin diversion takes place from Lake Michigan at Chicago. Here water is diverted from the Great Lakes to the Mississippi River basin. The water from Lake Huron flows through the St. Clair River, Lake St. Clair, and Detroit River system into Lake Erie. From Lake Erie the flow continues through the Niagara River and Welland Canal diversion into Lake Ontario. The Welland Canal diversion is an intrabasin diversion bypassing Niagara Falls and is used for navigation and hydropower production. There is also a small diversion into the New York State Barge Canal system which is ultimately discharged into Lake Ontario. From Lake Ontario, water flows through the St. Lawrence River to the Gulf of St. Lawrence and the Atlantic Ocean.

The hydrologic cycle of the Great Lakes basin and meteorology determine the net basin water supples to the lakes (runoff and precipitation less evaporation). Runoff comprises a significant part of the Great Lakes net basin supplies, particularly during the snowmelt season, late March through early June. Because the lakes are so large, lake precipitation and evaporation are of the same order of magnitude as runoff. On a monthly scale, precipitation is fairly uniformly distributed throughout the year. Lake evaporation typically has the greatest effect on net basin supplies during the winter months when dry air and warm water result in massive evaporation. Condensation on the cool lake surface from the wet overlying air occurs in the

summer. Net groundwater flows to each of the Great Lakes are generally negligible. Net basin supplies typically are maximum in late spring and minimum in late fall.

As water temperatures generally peak in August (September for Superior) at 15-25 °C and drop to freezing or near-freezing during the winter, the water column in each lake "turns over" (deep lower-density waters rise and mix with heavier surface layers) twice a year as surface temperature passes through that of maximum density for water (about 4 °C). There is also extensive ice cover on most of the lakes during most winters. The large heat storage of the deep lakes forestalls and reduces ice formation as well as shifts the large evaporation response to fall and winter.

GREAT LAKES PHYSICAL PROCESS MODELS

The Great Lakes Environmental Research Laboratory developed, calibrated, and verified conceptual model-based techniques for simulating hydrological processes in the Laurentian Great Lakes (including Georgian Bay and Lake St.Clair, both as separate entities). GLERL integrated the models into a system to estimate lake levels, whole-lake heat storage, and water and energy balances for forecasts and for assessment of impacts associated with climate change (Croley, 1990, 1993a,b; Croley and Hartmann, 1987, 1989; Croley and Lee, 1993; Hartmann, 1990). These include models for rainfall-runoff [121 daily watershed models (Croley, 1982, 1983a,b; Croley and Hartmann, 1984)], over-lake precipitation (a daily estimation model), one-dimensional (depth) lake thermodynamics [7 daily models for lake surface flux, thermal structure, and heat storage (Croley, 1989a,b, 1992a; Croley and Assel, 1993)], channel routing [4 daily models for connecting channel flow and level, outlet works, and lake levels (Hartmann, 1987, 1988; Quinn, 1978)], lake regulation [a monthly plan balancing Lakes Superior, Michigan, and Huron (International Lake Superior Board of Control, 1981, 1982) and a quarter-monthly plan balancing Lake Ontario and the St. Lawrence Seaway (International St. Lawrence River Board of Control, 1963)], and diversions and consumptions (International Great Lakes Diversions and Consumptive Uses Study Board, 1981).

Runoff Modeling

The GLERL Large Basin Runoff Model (LBRM) is an interdependent tank-cascade model which employs analytic solutions of climatologic considerations relevant for large watersheds (Croley, 1983a,b). It consists of moisture storages arranged as a serial and parallel cascade of "tanks" to coincide with the perceived basin storage structure of Fig. 1. Water enters the upper soil zone tank and flows from the upper to the lower soil zone and surface storage tanks, from the lower to the groundwater and surface tanks, from the groundwater to the surface tank, and from the surface tank out of the watershed.

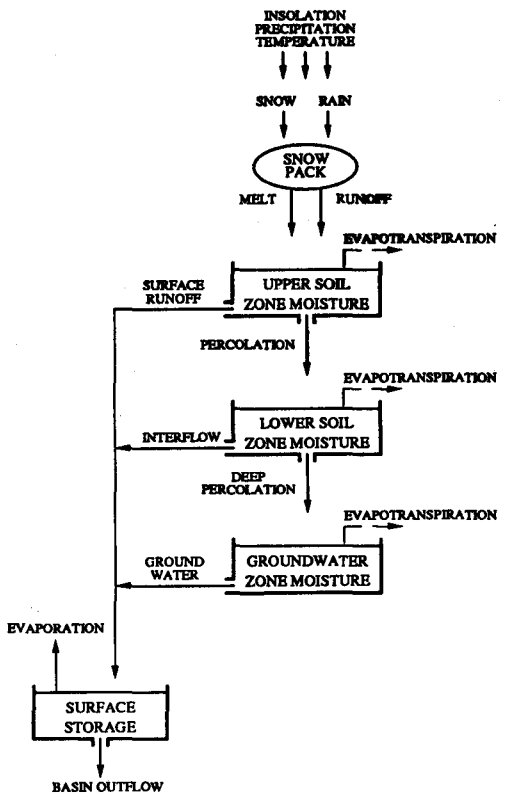

Fig. 1. Large Basin Runoff Model Tank-Cascade Conceptual Schematic.

Snowmelt and Infiltration. Water enters the snowpack, if present, and some then infiltrates into the upper soil zone based on degree-day determinations of snowmelt and net supply:

$$m_p = 0, \qquad T_a \le 0,$$
$$= a_s \, DD, \quad T_a > 0 \qquad (1)$$

where m_p = daily potential snowmelt rate ($m^3\ d^{-1}$); a_s = proportionality constant for snowmelt per degree-day ($m^3\ °C^{-1}\ d^{-1}$]); T_a = air temperature, estimated as the average of the daily maximum and minimum air temperatures (°C); and DD = degree-days per day (°C d d^{-1}), computed as the integral of air temperature with time over those portions of the day when it is positive. Since

the fluctuation of air temperature during the diurnal cycle is unknown, a triangular distribution is assumed (to approximate an expected sinusoidal variation) for ease of computation. The resulting expression for degree-days is:

$$\begin{aligned} DD &= 0, & T_{max} \le 0, \\ &= T_{max}^2 / (T_{max} - T_{min}) / 2, & T_{min} < 0 < T_{max}, \\ &= T_a, & 0 \le T_{min} \end{aligned} \quad (2)$$

where T_{max} = maximum daily air temperature (°C) and T_{min} = minimum daily air temperature (°C). Actual snowmelt depends upon the snowpack:

$$\begin{aligned} m &= m_p, & m_p d \le SNW_0, \\ &= SNW_0 / d, & m_p d > SNW_0 \end{aligned} \quad (3)$$

where m = daily snowmelt rate ($m^3 d^{-1}$) and SNW_0 = water content of the snowpack at the beginning of the day (m^3). Snowpack mass balance and water supply to the watershed surface can now be determined:

$$\begin{aligned} \frac{\delta}{\delta t} SNW &= p, & T_a \le 0, \\ &= -m, & T_a > 0 \end{aligned} \quad (4)$$

$$\begin{aligned} ns &= 0, & T_a \le 0, \\ &= p + m, & T_a > 0 \end{aligned} \quad (5)$$

where t = time, p = precipitation rate ($m^3 d^{-1}$), and ns = daily net supply rate to watershed surface ($m^3 d^{-1}$).

Heat Available for Evapotranspiration. The heat available for evapotranspiration is estimated empirically from the average air temperature as follows:

$$\Psi = K \exp(T_a / T_b) \quad (6)$$

where Ψ = total heat available for evapotranspiration during the day (cal), K = units and proportionality constant (cal), and T_b = a base scaling temperature (°C). The constant, K, is determinable from the following boundary constraint on the long-term heat balance:

$$\Sigma \Psi_i = \Sigma (rr_i - m_i \rho_w \gamma_f) d \quad (7)$$

where rr = daily solar insolation at the watershed surface (cal d^{-1}), ρ_w = density of water (= 10^6 gm m^{-3}), γ_f = latent heat of fusion (= 79.7 cal gm^{-1}), and the subscript, i, refers to daily values. Equation 7 conserves energy in that all absorbed insolation not used for snowmelt appears sooner or later as other components of the heat balance that determine Ψ. Daily insolation is taken as:

$$rr = 10000 A_b \tau (b_1 + b_2 X) \quad (8)$$

where A_b = area of the watershed (m^2), τ = daily extra-terrestrial solar radiation (langleys d^{-1}), b_1 and b_2 = constants, and X = daily ratio of hours of bright sunshine to maximum possible hours of bright sunshine, estimated from daily air temperatures:

$$X = MIN\{(T_{max} - T_{min}) / 15, 1.0\} \quad (9)$$

While calculations for ns and Ψ are performed on a daily basis, the mass balance computations (following) are performed on an n-day basis (n = 1, 7, and 28-31 are typical). The net supply and energy available for evapotranspiration are summed over the n-day periods prior to the mass balance:

$$ns_a = \frac{1}{n} \sum_{i=1}^{n} ns_i \quad (10)$$

$$\Psi_a = \sum_{i=1}^{n} \Psi_i \quad (11)$$

where ns_a = average net supply rate for n days ($m^3 d^{-1}$), Ψ_a = accumulated energy available for evapotranspiration over n days (cal), and n = number of days in the mass balance computation periods. The subscripts refer to daily values within the computation period.

Infiltration. Infiltration is taken as instantaneously proportional to the supply rate and to the areal extent of the unsaturated portion of the upper soil zone (partial-area infiltration concept).

$$f = ns_a (USZC - USZM) / USZC \quad (12)$$

where f = infiltration rate ($m^3 d^{-1}$), USZC = capacity of the upper soil zone (m^3), and USZM = content of upper soil zone (m^3). The difference between the net supply rate and infiltration is surface runoff in Fig. 1.

Evapotranspiration. All incoming heat is considered here to be released by the watershed surface by ignoring heat storage and the energy advected by evaporation. It consists of short-wave reflection, atmospheric heating (composed of net long wave exchange, sensible heat exchange, net atmospheric advection, and net hydrospheric advection), and evaporation-evapotranspiration (referred to herein jointly as evapotranspiration). The total heat available for evapotranspiration over a day is composed of the heat actually used for evapotranspiration and that used for atmospheric heating. At any instant, the rate of evaporation or evapotranspiration, e, is proportional to the amount of water available, Z (reflecting both areal coverage and extent of supply), and to the rate of nonlatent heat released to the atmosphere, $\delta H_s/\delta t$ (atmospheric heating):

$$e = \beta Z e_p, \quad e_p = \frac{\delta H_s}{\delta t} / (\rho_w \gamma_v) \tag{13}$$

where e = evaporation or evapotranspiration rate (m^3 d^{-1}), β = partial linear reservoir coefficient (m^{-3}), Z = volume of water in storage (m^3), e_p = rate of evaporation or evapotranspiration, respectively (m^3 d^{-1}), still possible and γ_v = latent heat of vaporization (596 - 0.52 T_a cal gm^{-1}). This agrees with existing climatologic and hydrologic concepts for evapotranspiration opportunity.

Over large areas, climatic observations suggest that actual evapotranspiration affects temperatures, wind speeds, humidities, and so forth, and hence it affects the potential evapotranspiration (evapotranspiration opportunity or capacity); the heat used for evapotranspiration reduces the opportunity for additional evapotranspiration (complementary evapotranspiration and evapotranspiration opportunity concept). This concept is modified here by considering that, for short time periods, the total amount of energy available for evapotranspiration, Ψ, during the time period is split into that used for evapotranspiration and that used for atmospheric heating. From (13), for the daily time period,

$$\Psi = H_s + \rho_w \gamma_v (E_u + E_l + E_g + E_s) \tag{14}$$

where H_s = nonlatent heat released to the atmosphere during the day (cal) and E_u, E_l, E_g, and E_s = evaporation or evapotranspiration from the upper soil zone, lower soil zone, groundwater, and surface storages (m^3), respectively. The evaporation from stream channels and other water surfaces (surface zone) in a large basin is very small compared to the basin evapotranspiration; groundwater evapotranspiration is also taken here as being relatively small.

Mass Conservation. Percolation from the upper zone enters the lower soil zone, and deep percolation from the lower zone enters the groundwater zone; see Fig. 1. Lateral flows from these zones of surface runoff, interflow, and groundwater flow, respectively, enter the surface storage zone which represents surface waters that ultimately flow from the basin. These flowrates are taken as instantaneously proportional to their respective storages (linear-reservoir flow concept). The mass balances for snowpack, upper and lower soil zones, groundwater, and surface water use these physically-based concepts, in the cascade of Fig. 1, to form a set of simultaneous ordinary linear differential equations whose joint solution depends upon the relative magnitude of all parameters, inputs, and system states (storages) pictured in Fig. 1.

$$\frac{\delta}{\delta t} USZM = ns_a (1 - USZM / USZC) - \alpha_{per} USZM - \beta_{eu} e_p USZM \tag{15}$$

$$\frac{\delta}{\delta t} LSZM = \alpha_{per} USZM - \alpha_{int} LSZM - \alpha_{dp} LSZM - \beta_{el} e_p LSZM \tag{16}$$

$$\frac{\delta}{\delta t} GZM = \alpha_{dp} LSZM - \alpha_{gw} GZM - \beta_{eg} e_p GZM \tag{17}$$

$$\frac{\delta}{\delta t} SS = ns_a USZM / USZC + \alpha_{int} LSZM + \alpha_{gw} GZM - \alpha_{sf} SS - \beta_{es} e_p SS \tag{18}$$

$$Q = \alpha_{sf} \int_0^{\Delta} SS \, \delta t \tag{19}$$

where α_{per} = percolation coefficient (d^{-1}), β_{eu} = upper zone evapotranspiration coefficient (m^{-3}), α_{int} = interflow coefficient (d^{-1}), LSZM = content of lower soil zone (m^3), α_{dp} = deep percolation coefficient (d^{-1}), β_{el} = lower zone evapotranspiration coefficient (m^{-3}), α_{gw} = groundwater coefficient (d^{-1}), GZM = content of groundwater zone (m^3), β_{eg} = groundwater zone evapotranspiration coefficient (m^{-3}), α_{sf} = surface outflow coefficient (d^{-1}), SS = content of surface storage zone (m^3), β_{es} = surface zone evapotranspiration coefficient (m^{-3}), Q = basin outflow volume for n days (m^3), and Δ = n times d. The value of e_p is determined by simultaneous solution of (15)-(19) and the following complementary relationship between actual evapotranspiration and that still possible from atmospheric heat, derived from (13) and (14):

$$\int_0^{\Delta} [e_p + (\beta_{eu} USZM + \beta_{el} LSZM + \beta_{eg} GZM + \beta_{es} SS) e_p] \, \delta t = \Psi_a / (\rho_w \gamma_v) \tag{20}$$

Analytical Solution. In the analytical solution, results from one storage zone are used in other zones where their outputs appear as inputs. There are 30 different analytic results, depending upon the relative magnitudes of the inputs (ns), the initial conditions ($USZM_0$, $LSZM_0$, GZM_0, SS_0, SNW_0), and the model parameters (T_b, α_s, α_{per}, β_{eu}, α_{int}, α_{dp}, β_{el}, α_{gw}, and α_{sf}) in (15)-(19) (note that β_{eg} and β_{es} are taken as zeroes). Complete analytic solutions for all possible ranges of values are available (Croley, 1982). Since the inputs and initial storages each day change from day to day, the appropriate analytic result, as well as its solution, varies with time; mathematical continuity between solutions is preserved however. Small parameter

values for a tank outflow imply small releases and large storage volumes; large values imply small storages and outflows nearly equal to inflows. The differential equations for the mass balances can be applied over any time increment by assuming that the input (precipitation and snowmelt) and heat available for evapotranspiration are uniform over the time increment. Thus, the resolution of the equations is limited only by the intervals over which precipitation and temperature data are available; numerical solutions are unnecessary so that approximation errors are avoided. Furthermore, solutions may proceed for either flow rates or storage volumes directly. The mass-balance computation interval may be any length greater than or equal to the interval length for which meteorologic data are available.

Application. The model is applied to daily data with either a fixed 1-d or a fixed 7-d mass-balance computation interval. Input and heat available for evapotranspiration are combined on a daily basis and summed over the interval as input to the mass-balance computations. The model is applied to monthly data with a variable mass-balance computation interval. The interval may represent 28 to 31 d, depending on the month and year. Input and heat available for evapotranspiration are computed over the same monthly interval. Data requirements include initial storage values, daily maximum and minimum air temperatures, daily precipitation, and for comparison purposes, daily basin outflow. Other data requirements are easily met. The mid-monthly extra-terrestrial solar radiation (from which daily values are interpolated) and the empirical constants, b_1 and b_2, are available in standard climatologic summaries. The area of the watershed is also required.

For application of the LBRM to a Great Lakes drainage basin, the basin is first divided into subbasins draining directly to the lake (there are 121 subbasins in the entire Great Lakes basin). The meteorologic data from typically 150-300 stations about and in the subbasins are combined through Thiessen weighting to produce areally-averaged daily time series of precipitation and minimum and maximum air temperatures for each subbasin. Weights are determined for each day of record, if necessary, since the data collection network changes frequently as stations are added, dropped, and moved or fail to report from time to time. This is feasible through the use of an algorithm for determining a Thiessen area-of-influence about a station by its edge [Croley and Hartmann, 1985]. Records for all "most-downstream" flow stations are combined by aggregating and extrapolating for ungauged areas to estimate the daily runoff to the lake from each subbasin. Thus, the LBRM is applied in a "distributed-parameter" application by combining model outflows from each of the subbasins to produce the entire basin runoff.

By combining the meteorologic and hydrologic data for all subbasins to represent the entire basin, the LBRM may be calibrated in a lumped-parameter application to the entire basin at one time. Although the application of lumped-parameter models to very large areas necessarily fails to represent areal distributions of watershed and meteorologic characteristics, spatial filtering effects tend to cancel data errors for small areas as the areas are added together. Distributed-parameter applications, in which the LBRM is calibrated for each subbasin and model outflows are combined to represent the entire basin, make use of information that is lost in the lumped-parameter approach; the integration then filters individual subbasin model errors.

There are five variables to be initialized prior to modeling: SNW, USZM, LSZM, GZM, and SS. While the initial snowpack, SNW_0, is easy to determine as zero during major portions of the year, these variables are generally difficult to estimate. If the model is to be used in forecasting or for short simulations, then it is important to determine these variables accurately prior to use of the model. If the model is to be used for calibration or for long simulations, then the initial values are generally unimportant. The effect of the initial values diminishes with the length of the simulation and after 1 year of simulation, the effects are nil from a practical point of view. Calibrations are repeated with initial conditions equal to observed long-term averages until there is no change in the averages to avoid arbitrary initial conditions when their effects do not diminish rapidly.

Calibration. We calibrate the LBRM for each subbasin with 30 years of daily weighted subbasin climatologic data. The nine parameters are determined (Croley and Hartmann, 1984) by searching the parameter space systematically, minimizing the root mean square error between model and actual outflows for each parameter, selected in rotation, until all parameters converge within two significant digits. Comparisons with other runoff models (Croley, 1983a) and climatology (Croley and Hartmann, 1984) show the LBRM to be far superior for estimates of runoff volumes from large basins.

The LBRM captures a "realism" in its structure that has several advantages over other models. Basin storages, modeled as "tanks", are automatically removed as respective parameters approach their limits. Thus, the structure of the model changes within a calibration. This is achieved without the use of "threshold" parameters in the model since physical concepts are used which avoid discontinuities in the goodness-of-fit as a function of the parameters; these concepts appear especially relevant for large-basin modeling. Because the "tanks" relate directly to actual basin storages, intialization of the model corresponds to identifying storages from field conditions which may be measured; interpretations of a basin's hydrology then can aid in setting both initial and boundary conditions. The tanks in Fig. 1 may be intialized to correspond to measurements of snow and soil moisture water equivalents available from aerial or satellite monitoring. Snow water equivalents are used in Lake Superior applica-

tions (Gauthier et al., 1984).

The LBRM calibration periods generally cover 1965-1982 depending upon flow data availability. Table 1 presents overall calibration results for the distributed-parameter applications. The LBRM was also used in forecasts of Lake Superior water levels (Croley and Hartmann, 1987), and comparisons with climatic outlooks showed the runoff model was very close to actual runoff (monthly correlations of water supply were on the order of 0.99) for the period August 1982 - December 1984 which is outside of and wetter than the calibration period (Croley and Hartmann, 1986). The model also was used to simulate flows for the time period 1956-63, outside of the period of calibration. The correlation of monthly flow volumes between the model and observed during this verification period are also contained in Table 1. They are a little lower than the calibration correlations but quite good except for Lakes Superior and Huron (there were less than two thirds as many flow gages available for 1956-63 as for the calibration period for these basins).

Studies on the Lake Ontario basin (Croley, 1982, 1983b) show that the simple search algorithm described herein does not give unique optimums for calibrated parameter sets because of synergistic relationships between parameters. However, the calibration procedure does show a high degree of repeatability for recalibrations with different starting values, and consistent parameter values are obtained for subbasins with similar hydrologic characteristics. On the other hand, the nonuniqueness of calibrated parameters was demonstrated by recalibrating for a synthetic data set. The model was calibrated for the entire Lake Superior basin and then used to simulate outflows to create a new data set for calibration. Subsequent calibration started with a very different initial parameter set and yielded an "optimum" parameter set different from the original with a relatively poor goodness-of-fit. If the original parameter set had been unique, the parameter values produced from the recalibration to the synthetic data set should have been the same as the parameters used to create that data set. This illustrates the nonuniqueness of the parameters, the importance of the starting values used in the search, and the problems inherent in searching the parameter space. Additionally, some components of the LBRM (such as linear reservoirs) are more likely to adequately represent their processes in the real world than other (such as degree-day melting or complementary evapotranspiration). Parameter estimation techniques that properly weight a model's more accurate parts could improve parameter estimates.

Over-Lake Precipitation

The lack of over-lake precipitation measurements means that estimates typically depend on land-based measurements and there may be differences between land and lake meteorology. Although gage exposures may significantly influence the results of lake-land precipitation studies (Bolsenga, 1977, 1979), Wilson (1977) found that Lake Ontario precipitation estimates based on only near-shore stations averaged 5.6% more during the warm season and 2.1% less during the cold season than estimates based on stations situated in the lake. By using a network that also included stations somewhat removed from the Lake Ontario shoreline, Bolsenga and Hagman (1975) found that eliminating several gages not immediately in the vicinity of the shoreline increased over-lake precipitation estimates during the warm season and decreased them during the cold season. Thus, for the Great Lakes, where lake effects on near-shore meteorology are significant and the drainage basins have relatively low relief, the use here of all available meteorologic stations throughout the basin is probably less biased than the use of only near-shore stations. Overlake precipitation is taken equal to overland precipitation (on the basis of depth) without further corrections.

Table 1. Large Basin Runoff Model Calibration Statistics[a].

Lake	Number of Sub-basins	Mean 1-day Flow (mm)[b]	Flow Std. Dev. (mm)[b]	Root Mean Square Error (mm)[b]	Correlation Calib.	Correlation Verif.
Superior	22	1.12	0.67	0.25	0.93	0.77
Michigan	29	0.89	0.47	0.18	0.93	0.86
Huron	27	1.06	0.69	0.26	0.92	0.69
St. Clair	7	0.90	1.36	0.62	0.89	0.87
Erie	21	1.01	1.28	0.54	0.91	0.90
Ontario	15	1.41	1.13	0.43	0.93	0.89

[a]Statistics and calibrations generally cover 1966-83; verification generally covers 1956-63.
[b]Equivalent depth over the land portion of the basin.

Over-Lake Evaporation

Great Lakes hydrologic research mandates the use of continuous-simulation models of daily lake evaporation over long time periods. Such models must be usable in the absence of water surface temperature and ice cover observations. They also must be physically based to have application under environmental conditions different than those under which they were derived. GLERL developed a lumped-parameter (point) model of evaporation and thermodynamic fluxes for the Great Lakes based on an energy balance at the lake's surface (Croley, 1989a,b) and on one-dimensional (vertical) lake heat storage (Croley, 1992a). Ice formation and loss is coupled also to lake thermodynamics and heat storage (Croley and Assel, 1993).

Thermodynamic Fluxes. The thermodynamic fluxes to and from a lake include incident shortwave radiation, q_i, reflected shortwave radiation, q_r and q_r' (over water and over ice, respectively), evaporative (latent and advected) heat transfer, q_e and q_e', sensible heat transfer, q_h and q_h', precipitation heat advection, q_p and q_p', net longwave radiation exchange, Q_l, and surface flow advection, Q_I; see Croley (1989a,b) for details:

$$q_i = [0.355 + 0.68\,(1 - N)]\,q_0 \qquad (21)$$

where q_i = daily average unit (per unit area) rate of shortwave radiation incident to the earth's surface, N = fraction of the sky covered by clouds, and q_0 = daily average unit rate of short-wave radiation received on a horizontal unit area of the Earth's surface under cloudless skies;

$$q_r = 0.1\,q_i \qquad (22)$$

where q_r = average unit reflected shortwave radiation rate from the water surface;

$$e_w = \rho_a C_E (q_w - q)\,U / \rho_w \qquad (23)$$

where e_w = over-water evaporation rate, ρ_a = density of air, C_E = bulk evaporation coefficient over water, q_w = specific humidity of saturated air at the temperature of the water surface, q = specific humidity of the atmosphere over water, and U = windspeed over water;

$$q_e = (\gamma_v + C_w T)\,e_w \rho_w \qquad (24)$$

where q_e = average unit evaporative (latent and advected) heat transfer rate from the water surface, C_w = specific heat of water, and T = water surface temperature;

$$q_h = \rho_a C_p C_H (T_a - T)\,U \qquad (25)$$

where q_h = average unit sensible heat transfer rate to the water surface, C_p = specific heat of air at constant temperature, and C_H = sensible heat coefficient over water;

$$q_p = (C_w T_a - \gamma_f)\,\rho_w p, \qquad T_a < 0°C$$
$$= C_w T_a \rho_w p, \qquad T_a \geq 0°C \qquad (26)$$

where q_p = average unit precipitation heat advection rate to the water surface;

$$q_\uparrow = \varepsilon_w \sigma (T + 273.16°C)^4 \qquad (27)$$

where $q_\uparrow$ = average unit longwave radiation emitted by the water body, σ = Stephan-Bolzman constant (5.67×10^{-8} W m^{-2} °K^{-1}), and ε_w = emissivity of the water surface;

$$q_\downarrow = (1 - r_a)\,\varepsilon_a \sigma (T_a + 273.16°C)^4 \qquad (28)$$

where $q_\downarrow$ = average unit longwave radiation from the atmosphere absorbed by the water surface and ε_a = emissivity of the atmosphere;

$$Q_l = \{q_\downarrow [\eta + (1 - \eta)(1 - N)] - q_\uparrow\}\,(A_w + A) \qquad (29)$$

where Q_l = average net longwave radiation exchange rate between the entire water body and the atmosphere (effects of ice cover on the net longwave exchange are ignored here), η = empirical coefficient relating cloudiness to atmospheric longwave radiation, A_w = area of the open-water (ice-free) surface, and A = area of the ice surface;

$$Q_I = \rho_w C_w T (\Theta_i - \Theta_o) \qquad (30)$$

where Q_I = daily net heat advection to the lake from overland flow and channel inputs and outputs, Θ_i = sum of all surface inflows to the lake, and Θ_o = sum of all outflows from a lake;

$$q_r' = (0.85\,f_n + 0.70\,f_o + 0.50\,f_m + 0.45\,f_b)\,q_i \qquad (31)$$

where q_r' = average unit reflected shortwave radiation rate from the ice pack, f_n = fraction of ice covered with new snow, f_o = fraction of ice covered with old snow, f_m = fraction of ice covered with melting snow, and f_b = fraction of ice that is bare of snow;

$$e_w' = \rho_a C_E' (q_w' - q')\,U' / \rho_w \qquad (32)$$

where e_w' = over-ice evaporation rate, C_E' = bulk evaporation coefficient over ice, q_w' = specific humidity of saturated air at temperature of ice, q' = specific humidity of the atmosphere over ice, and U' = windspeed over ice;

$$q_e' = (\gamma_v + \gamma_f + C_w T') e_w' \rho_w \quad (33)$$

where q_e' = average unit evaporative (latent and advected) heat transfer rate from the ice pack and T' = ice surface temperature;

$$q_h' = \rho_a C_p C_H' (T_a' - T') U' \quad (34)$$

where q_h' = average unit sensible heat transfer rate to the ice pack, C_H' = sensible heat coefficient over ice, and T_a' = temperature of the air over ice; and

$$q_p' = C_w T_a' \rho_w p \quad (35)$$

where q_p' = average unit precipitation heat advection rate to the ice pack.

Gray et al. (1973) provided (21), generalized maps of mid-monthly values from which q_0 may be interpolated by date, and the shortwave reflection of (22) and (31). Because data are unavailable and because subsequent heat budgets are insensitive to their values, f_n, f_o, and f_m are set to zero here and f_b is set to unity. Values of over-water and over-ice meteorology (q, U, T_a, N, q', U', and T_a') are determined from overland values by adjusting for over-water conditions. Phillips' and Irbe's (1978) regressions for over-water corrections are used directly by replacing the fetch (and derived quantities) with averages. The bulk evaporation coefficients over water and over ice (C_E and C_E') are determined similar to Quinn (1979) from over-water or over-ice (respectively) windspeed, air temperature, and surface temperature. The over-water and over-ice sensible heat coefficients (C_H and C_H') are taken equal to the bulk evaporation coefficients, respectively (Quinn, 1979). The emissivities of water and air in (27) and (28) [note the reflectivity of the water surface in (28) is $r_a = 1 - \varepsilon_w$] are taken, respectively, as 0.97, and $0.53 + 0.065\, e_a^{1/2}$ where e_a is the vapor pressure of the air (mb) after Keijman (1974). Temperatures in (27) and (28) are absolute (°K).

Heat Storage. The heat added to a lake and the heat added to the ice pack, from the surface fluxes, are governed by simple energy and mass balances, energy-storage relationships, and boundary conditions on ice growth, water temperature, and ice temperature; see Fig. 2. The rate of change of heat storage in a lake with time is:

$$\frac{\delta H}{\delta t} = A_w (q_i - q_r - q_e + q_h + q_p) + Q_l + Q_I - Q_w \quad (36)$$

where $\delta H/\delta t$ = time rate of change of heat storage H in the lake and Q_w = total heat flux between the water body and the ice pack. The rate of change of heat storage in the ice pack with time is defined here as:

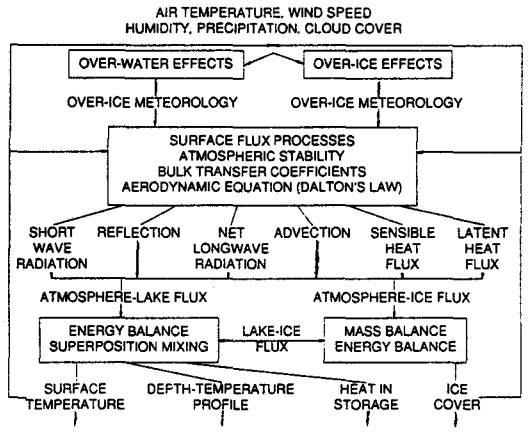

Fig. 2. Large Lake Thermodynamic Fluxes and Heat Storage Model Schematic.

$$\frac{\delta H'}{\delta t} = A (q_i - q_r' - q_e' + q_h' + q_p') + Q_w \quad (37)$$

where $\delta H'/\delta t$ = time rate of change of heat storage H' in the ice pack.

Kraus and Turner's (1967) mixed-layer thermal structure concept is extended for the Great Lakes to allow the determination of simple heat storage. The effects of past additions or losses are superimposed to determine the surface temperature on any day as a function of heat in storage; each past addition or loss is parameterized by its age. Turnovers (convective mixing of deep lower-density waters with surface waters as surface temperature passes through that at maximum density) can occur as a fundamental behavior of this superposition model and hysteresis between heat in storage and surface temperature, observed during the heating and cooling cycles on the lakes, is preserved. Water surface temperature becomes (Croley, 1992a):

$$T_k = 3.98°C + \sum_{m=1}^{k} f_{k,m} \left(\min_{m \le n \le k} H_n - \min_{m-1 \le n \le k} H_n \right) \quad (38)$$

where T_k = water surface temperature and H_k = heat storage in the lake k days after the last turnover, and $f_{k,m}$ is a "wind-aging" function, defined subsequently, relating surface temperature rise on day k to heat added on day m. Ice pack surface temperature is related to ice pack heat storage here as:

$$H'_k = \rho C_i V_k T'_k / 2 - \rho \gamma_f V'_k \quad (39)$$

where T'_k = ice surface temperature on day k, H'_k = heat storage in the ice pack on day k, ρ = density of ice, C_i = specific heat of ice, V_k = volume of the ice pack on day k, and V'_k = volume of ice formed by freezing or melting on day k. The boundary conditions on water surface temperature and volume of the ice pack for every day (dropping the daily subscript) are:

$$V = 0, \qquad T \geq 0°C \quad (40)$$

$$T = 0°C, \qquad V \geq 0 \quad (41)$$

These equations are satisfied by selecting the heat flux between the water and ice, Q_w, appropriately. Q_w, if negative, is yielded as ice forms (to keep water surface temperature from going below freezing) and, if positive, is used in melting ice (to keep water surface temperature at freezing as long as there is ice present). The boundary conditions on ice surface temperature and volume of the ice pack for every day (dropping the daily subscript) are:

$$T' = T_a, \qquad V > 0 \text{ and } T_a \leq 0°C \quad (42)$$

$$T' = 0°C, \qquad V = 0 \text{ or } T_a > 0°C \quad (43)$$

where T_a = over-ice air temperature. The volume of the ice pack, V, and the volume of ice formed by freezing or melting, V', are related:

$$\frac{\delta V}{\delta t} = \frac{\delta V'}{\delta t} + S - E \quad (44)$$

where S = volumetric rate of snow falling on the ice and E = volumetric rate of evaporation from the ice. The "wind-aging" function, $f_{k,m}$, is:

$$f_{k,m} = \frac{2 - M_{k,m}/F}{\rho_w C_w M_{k,m}}, \quad M_{k,m} < \mathrm{MIN}\left(F, \frac{2 V_c}{1 + V_c / F}\right)$$

$$= \frac{1}{\rho_w C_w M_{k,m}}, \quad M_{k,m} \geq \mathrm{MIN}\left(F, \frac{2 V_c}{1 + V_c / F}\right)$$

$$\text{and } M_{k,m} < \mathrm{MAX}\left(V_c, \frac{2 V_c}{1 + V_c / F}\right)$$

$$= \frac{1}{\rho_w C_w V_c}, \quad M_{k,m} < \mathrm{MAX}\left(V_c, \frac{2 V_c}{1 + V_c / F}\right) \quad (45)$$

where V_c = volume (capacity) of the lake and $M_{k,m}$ = mixing volume size in the lake, on day k, of the heat added on day m (a function of accumulated wind movement, W_j, from day m through day k),

$$M_{k,m} = V_e \left[1 + a \,\mathrm{EXP}\left(-b \sum_{j=m}^{k} W_j\right)\right]^{-1} \quad (46)$$

Also, a, b, F, and V_e = empirical parameters to be determined in a calibration to observed data. V_e is interpreted as the "equilibrium" volume approached as a limit (in a sufficiently deep lake) since the effects of wind mixing at the surface diminish with distance from the surface. F is interpreted as the mixing volume at which a heat addition is fully mixed throughout. Parameters a, b, and F are defined for water temperatures above 3.98°C ("turnover" temperature of water at maximum density) and are replaced by a', b', and F', respectively, for water temperatures below 3.98°C. Details for the flux terms in (36) and (37) are presented by Croley (1989a,b). Derivation details of (38), (45), and (46) are available elsewhere (Croley, 1992a).

Ice Pack Growth. In (39), linear vertical temperatures are used through the ice pack from T' on the surface to 0°C on the bottom, similar to Green and Outcalt (1985). Differentiating (4) and ignoring small terms,

$$\frac{\delta H'}{\delta t} \cong \frac{1}{2} \rho C_i V \frac{\delta T'}{\delta t} - \rho \gamma \frac{\delta V'}{\delta t} \quad (47)$$

Thus, the heat change is split between a temperature change in the ice pack and a volume change due to melting or freezing. Comparing (37) and (47), note the temperature change in (47) is taken here as resulting from a portion of the heat added from (or lost to) the atmosphere $[A (q_i - q'_r - q'_e + q'_h + q'_p)]$. The remainder of that heat is identified as Q_a:

$$Q_a = A (q_i - q'_r - q'_e + q'_h + q'_p) - \frac{1}{2} \rho C_i V \frac{\delta T'}{\delta t} \quad (48)$$

This heat (Q_a) and all of the heat added from the water body, Q_w, then result in changes to the ice pack volume (freezing or melting); from (37), (44), (47), (48):

$$Q_a + Q_w = -\rho \gamma \frac{\delta V'}{\delta t} = -\rho \gamma \left(\frac{\delta V}{\delta t} - S + E\right) \quad (49)$$

Consider a prismatic ice pack with surface area A and depth (or thickness) D. The heat exchange between the atmosphere and the ice pack available for freezing or melting, Q_a, is taken as resulting in either melt (along the entire atmosphere-ice surface) or freezing (along

the entire water-ice surface). The heat exchange between the water body and the ice pack, Q_w, is taken as resulting in changes along only the water/ice surface (either melt or freezing). After simplification (Croley and Assel, 1993),

$$\frac{\delta D}{\delta t} = \left\{ -\frac{Q_a}{A + x_w D} I_{(-\infty,\, 0]}(Q_a) - \frac{Q_a}{A + x_a D} I_{(0,\, \infty)}(Q_a) - \frac{Q_w}{A + x_w D} \right\} \frac{1}{\rho \gamma} + \frac{S}{A} - \frac{E}{A + x_a D} \tag{50}$$

$$\frac{\delta A}{\delta t} = \left\{ -\frac{x_w Q_a}{A + x_w D} I_{(-\infty,\, 0]}(Q_a) - \frac{x_a Q_a}{A + x_a D} I_{(0,\, \infty)}(Q_a) - \frac{x_w Q_w}{A + x_w D} \right\} \frac{1}{\rho \gamma} - \frac{x_a E}{A + x_a D} \tag{51}$$

$$x_a = \tau_a A^{1/2} \tag{52}$$

$$x_w = \tau_w A^{1/2} \tag{53}$$

where $I_{(-\infty)}(x)$ = indicator function (equal to unity if the quantity in parentheses, x, is within the indicated interval and equal to zero if not), τ_a and τ_w = empirical coefficients depending upon ice pack shape, the ratios of vertical to lateral changes along the atmosphere-ice interface and along the water-ice interface, and the buoyancy of ice. The change in total ice volume is, from (50) and (51):

$$\frac{\delta V}{\delta t} = \frac{\delta(A\,D)}{\delta t} = A \frac{\delta D}{\delta t} + D \frac{\delta A}{\delta t} = \{-Q_a - Q_w\} \frac{1}{\rho \gamma} + S - E \tag{54}$$

Note (49) and (54) agree.

Equations (36)-(48), (50)-(54), and those for the component fluxes, (21)-(35), may be solved simultaneously to determine the heat storage, the water and ice surface temperatures, and the ice pack extents.

Calibration Procedure. Two calibrations are involved in applying the model in a particular setting. The first determines the first eight parameters (a, b, F, a', b', F', V_e, and η). The first seven parameters relate to superposition heat storage (Croley, 1992a) and the eighth parameter, η, reflects the effect of cloudiness on the atmospheric net longwave radiation exchange (Croley, 1989a,b). This calibration minimizes daily water surface temperature root mean square error (RMSE) by using methods described elsewhere (Croley and Hartmann, 1984). Meteorology data for 1948-1985 and water surface temperature data on each of the Great Lakes, except Lake Michigan, were taken from airplane and satellite measurements, extended through August 1988, and prepared as described by Croley (1989a,b). Water surface temperature data for Lake Michigan from 1981 through 1985 were gleaned from areal maps prepared at the National Weather Service's Marine Predictions Branch (B. Newell, personal communication, 1990) and extended through August 1988 also. The second calibration determines the two parameters (τ_a and τ_w) that minimize daily ice cover RMSE with these same calibration techniques. Lake-averaged ice cover for model calibration was calculated from GLERL's digital ice cover data base (Assel, 1983). In most cases, less than 100% of a lake was observed on any given date. If less than 70% of the Lake Superior surface was observed, the ice cover for that date was not included in the model calibration. A subjective estimate of lake-averaged ice cover was made for the other Great Lakes if the data were insufficient.

Parameters are determined, in both cases, in automated systematic searches of the parameter spaces to minimize the RMSE between simulated and model outputs. Each parameter, selected in rotation, is searched until all parameter values converge to four digits, instead of searching only until the RMSE stabilizes. This simple search algorithm does not give unique optima for calibrated parameter sets because of synergistic relationships between parameters which allow parameter compensations to occur. However, the model concepts have been carefully chosen so that the parameters have physical significance; this allows them to be interpreted in terms of the thermodynamics they represent. Initialization of the model corresponds to identifying values from field conditions which may be measured; interpretations of a lake's thermodynamics then can aid in setting both initial and boundary conditions.

Prior to calibration or model use, the (spatial) average temperature-depth profile in the lake and the ice cover must be initialized. While the ice cover is easy to determine as zero during major portions of the year, the average temperature-depth profile in the lake is generally difficult to determine. If the model is to be used in forecasting or for short simulations, then it is important to determine these variables accurately prior to use of the model. If the model is to be used for calibration or for long simulations, then the initial values are generally unimportant. The effect of the

initial values diminishes with the length of the simulation, and after 2-3 years of simulation, the effects are nil from a practical point of view.

Empirical coefficients of the evaporation, heat storage, and ice sub-models were calibrated in an iterative process that used the two calibrations sequentially in rotation. We used independent data (lake-averaged daily surface temperature for the lake thermodynamics and heat storage sub-models and lake-averaged daily ice cover for the lake ice cover sub-model). First we minimized the RMSE of daily water surface temperature by calibrating lake thermodynamics model parameters and holding the parameters for the ice cover sub-model constant. We then held lake thermodynamics model parameters constant and calibrated the parameters of the ice cover sub-model to minimize the RMSE of daily ice cover. Then we repeated the process until the RMSEs for both water surface temperatures and ice cover were not significantly reduced from the previous iteration. The results are summarized in Table 2.

Turnovers (convective mixing of deep lower-density waters with surface waters as surface temperature passes through that at maximum density) occur as a fundamental behavior of GLERL's thermodynamic and heat storage model. Hysteresis between heat in storage and surface temperature, observed during the heating and cooling cycles on the lakes, is preserved. The model also correctly depicts lake-wide seasonal heating and cooling cycles, vertical tempertaure distributions, and other mixed-layer developments. There is good agreement between the actual and calibrated-model water surface temperatures; the RMSE is between 1.1-1.6 °C on the large lakes [within 1.1-1.9 °C for an independent verification period, 1966-78 (Croley, 1989a,b, 1992a)]. There is also good agreement with 8 years of bathythermograph observations of depth-temperature profiles on Lake Superior and 1 year of independently-derived weekly or monthly surface flux estimates on Lakes Superior, Erie, and Ontario (2 estimates).

Calibration Issues. There were several problems in calibrating the model. First, it appears that the models are close to being over-specified in terms of the number of parameters used; i.e., there appear to be almost too many degrees of freedom allowed for the data sets used in the calibrations. The result is that the optimums are not unique and it is not possible to determine meaningful values of any additional parameters. Parameter compensation exists so that changes in one parameter can be offset by changes in other parameters with little change in the RMSE of the calibration. This made it difficult to determine an ice break-up model, not presented here, which had an additional three parameters. We had considered ice breakage and rejoining by developing a differential equation for the rate of change with time of the number of ice pieces as a function of wind stress, melting, and refreezing. We could not meaningfully calibrate this addition to the ice model with the ice cover data sets we had, and so we eliminated ice break-up from the model presented here. Perhaps when other parameters are reduced through model reformulations in calibrations at a later date, it will be possible to model and calibrate for ice break-up in a meaningful manner.

Second, optimizing parameters with regard to two objectives (minimizing RMSEs associated with water surface temperatures and ice cover) does not produce the same parameter sets. There seems to be a trade-off between the two objectives at times and RMSE of water temperatures decreases at the expense of ice cover RMSE and vice-versa.

The model has ten parameters calibrated to match water surface temperatures and ice cover. Seven of them are defined in the superposition heat storage submodel. The number of empirical model parameters could perhaps be reduced by use of other one-dimensional mixed-layer heat-storage models (McCormick and Meadows, 1988; Hostetler and Bartlein, 1990). The critical limitation of such models for long-term hydrological forecasting and simulation is the lack of representative or accurate hourly hydrometeorological data over long periods. Secondarily, computer time can be excessive for such models in forecast or multi-year simulation environments.

Models Applicability

Although GLERL uses a daily resolution of data with their models, basin-wide processes of runoff, over-lake precipitation, and lake evaporation (described with models here) respond discernably to weekly changes at best, and monthly is usually adequate for net supply and lake level simulation (this ignores short-term fluctuations associated with storm movement which are not addressed in this study). Likewise, spatial resolution finer than about 1000-5000 km^2 (the present average resolution of GLERL's models and their applications) is unnecessary, for use with general circulation models (GCMs) of the atmosphere, and much can be done in assessing hydrology changes at resolutions of 100,000 - 1,000,000 km^2 with lumped versions of the models. This coarse spatial resolution is still much finer than present GCM grids.

The models were assessed partially by computing net basin supplies to the lakes (basin runoff plus overlake precipitation minus overlake evaporation) with historical meteorological data for 1951-80 and comparing to historical net basin supplies. The absolute average annual difference ranged from 1.6% to 2.7% on the deep lakes, while the Lake St. Clair and Lake Erie applications were 12.0% and 7.0% respectively; month-to-month differences showed more variation. These differences generally reflect poorer evaporation modeling on the shallow lakes and snowmelt and evapotranspiration model discrepancies for the other lake basins. While monthly differences were generally small, a few were significant. The low annual residuals were felt to

Table 2. Daily Lake Evaporation Model Calibration Results.

	Lake					
	Superior	Michigan	Huron	Georgian	Erie	Ontario
CALIBRATION PERIOD STATISTICS						
Water Surface Temperatures (1980-88)[a]						
Means Ratio[b]	1.00	1.01	0.98	1.01	1.03	0.99
Variances Ratio[c]	1.01	0.98	0.95	1.02	1.08	0.99
Correlation[d]	0.98	0.97	0.98	0.99	0.99	0.98
R. M. S. E.[e]	1.13	1.56	1.33	1.10	1.58	1.43
Ice Concentrations (1960-1988)[f]						
Means Ratio[g]	0.92	0.72	0.70	0.98	1.15	0.39
Variances Ratio[h]	1.24	1.02	1.67	1.62	1.09	0.63
Correlation[i]	0.76	0.83	0.73	0.77	0.89	0.54
R. M. S. E.[j]	23.4	12.4	26.0	21.5	19.0	15.4
VERIFICATION PERIOD STATISTICS						
Water Surface Temperatures (1966-79)[k]						
Means Ratio[b]	0.96		1.03	0.98	1.05	0.94
Variances Ratio[c]	1.10		0.95	1.00	1.10	0.97
Correlation[d]	0.97		0.99	0.98	0.98	0.96
R. M. S. E.[e]	1.09		1.10	1.34	1.91	1.92

[a]Data between January 1, 1980 and August 31, 1988 for all lakes except Michigan and between January 1, 1981 and August 31, 1988 for Lake Michigan, with an initialization period for all lakes except Georgian Bay starting January 1, 1948 and January 1, 1953 for Georgian Bay.
[b]Ratio of mean model surface temperature to data mean.
[c]Ratio of variance of model surface temperature to data variance.
[d]Correlation between model and data surface temperature.
[e]Root-mean-square error between model and data surface temperatures in degrees C.
[f]Data between January 1, 1960 and August 31, 1988 for all Great Lakes except Superior and between March 1, 1963 and August 31, 1988 for Lake Superior, with an initialization period for all lakes starting January 1, 1958.
[g]Ratio of mean model ice concentration to data mean.
[h]Ratio of variance of model ice concentration to data variance.
[i]Correlation between model and data ice concentration.
[j]Root-mean-square error between model and data ice concentrations in %.
[k]Data between January 1, 1966 and December 31, 1979 for all lakes except Michigan with an initialization period for all lakes except Georgian Bay starting January 1, 1948 and January 1, 1953 for Georgian Bay.

be acceptable for use of these models in assessing changes from the current climate as they would be consistently applied to both a "present" and a "changed" climate. Further assessment of model deficiencies with comparisons to historical net basin supplies is difficult since the latter are derived from water budgets which incorporate all budget term errors in the derived net basin supplies.

There is some indication of model applicability outside of the time periods over which the models were calibrated as indicated above and in Tables 1 and 2. To assess the applicability of the process models to a climate warmer than the one under which they were calibrated and verified requires access to meteorologic data and process outputs for the warmer climate which unfortunately do not exist. Warm periods early in this

century are not sufficiently documented for the Great Lakes. In particular, data are lacking on watershed runoff to the lakes, water surface temperatures, windspeed, humidity, cloudcover, and solar insolation.

It is entirely possible that the models are tied somewhat to the present climate; empiricism is employed in the evapotranspiration component of the LBRM and in some of the heat flux terms in the heat balance and lake evaporation model. Coefficients were determined or selected in accordance with the present climate. The models are all based on physical concepts that should be good under any climate; however, the assumption is made that they represent processes under a changed climate that are the same as the present ones. These include linear reservoir moisture storages, partial-area infiltration, lake heat-storage relations with surface temperature, and gray-body radiation. However, the calibration and verification periods for the component process models include a range of air temperatures, precipitation, and other meteorological variables that encompass much of the changes in these variables predicted for a changed climate. Even though the changes are transitory in the calibration and verification period data sets, the models appear to work well under these conditions.

GREAT LAKES CLIMATE CHANGE RESPONSE

Methodology

GLERL constructed a master computer procedure to integrate the Large Basin Runoff Model, over-lake precipitation estimates, and the lake evaporation models for all lakes to provide a net water supply model for the entire Great Lakes system. They developed it specifically to look at the impact of changed climate by doing simulations with changed meteorology that represent scenarios of changed climate and comparing with simulations based on historical meteorology (representing an unchanged climate). Inputs are areal-average daily precipitation and maximum and minimum air temperatures for each of the 121 watersheds about the Great Lakes and areal-average daily air temperature, cloudcover, humidity, and windspeed for each of the five Great Lakes and Lake St. Clair.

GLERL's general procedure for the investigation of steady-state behavior under a changed climate is similar to that used for the EPA, as detailed elsewhere (Croley, 1991; Louie, 1991); it required that GLERL first simulate 38 years of "present" hydrology by using historical daily maximum and minimum air temperatures, precipitation, windspeed, humidity, and cloud cover data for the 1951-88 period; this is called the "base case" or "1xCO_2" scenario. The initial conditions were arbitrarily set but an initialization simulation period of 1 January 1948 through 31 December 1950 was used to allow the models to converge to conditions (basin moisture storages, water surface temperatures, and lake heat storages) initial to the 1 January 1951 through 31 December 1988 period. GLERL then attempted to estimate "steady-state" conditions, but there were problems.

The procedure to estimate "steady-state" conditions is to repeat the 41-yr simulation with initial conditions (basin moisture storages, lake heat storages, and surface temperatures) set equal to their values at the end of the simulation period, until they are unchanging. This procedure requires many iterations for a few subbasins with very slow groundwater storages and suggests very different initial groundwater storages than were used in calibrations. Actually, the original calibrations of the models used arbitrary (but fixed) initial conditions. GLERL should have determined initial conditions also in the calibrations, but that was unfeasible; there is little confidence in calibrated parameter sets that suggest very slow groundwater storages (half-lives on the order of several hundred years in some cases) since only 10 to 20 years were used in the calibrations. Therefore, the best estimate of "present" hydrology is to use calibrated parameters with initial conditions on "the same order" as those assumed for the calibrations. GLERL did the latter and then conducted simulations with adjusted data sets.

Average monthly absolute air temperatures, specific humidities, cloudcover, precipitation, and windspeed were supplied for each month of the year by the Canadian Climate Centre as resulting from their second-generation global circulation model (CCCGCMII); see McFarlane (1991) and McFarlane et al. (1991). While available at grid points spaced 3.75 degrees latitude by 3.75 degrees longitude, Louie (1991) interpolated monthly averaged data to a grid of 1 degree latitude by 1 degree longitude for both the "present" and "future" atmospheres (with one and two times the CO_2 content of the "present" atmosphere). He weighted values at surrounding grid points inversely to the square of the distance to each point. GLERL computed ratios of "future" (2xCO_2) to "present" (1xCO_2) monthly average absolute air temperatures, specific humidities, cloudcover, and precipitation and monthly average differences of 2xCO_2 to 1xCO_2 windspeeds at each of these gridpoints. They then used these ratios and differences with the historical data to estimate the 41-year sequences (1948-88) of atmospheric conditions associated with a changed climate, referred to as the "2xCO_2" scenario.

GLERL inspected each of the 770,000 square kilometers within the Great Lakes basin to see which gridpoint it is closest to and applied the monthly adjustment at that gridpoint to data representing that square kilometer. By combining all square kilometers representing a watershed or the lake surface, GLERL derived an areally-averaged adjustment to apply to their areally-averaged data sets for the watershed or lake surface, respectively. They then used the 2xCO_2 scenario in simulations similar to the base case scenario. They repeated the 41-yr simulation with initial conditions set equal to their values at the end of

the simulation period, until they were unchanging to estimate "steady-state" future conditions. They then interpreted differences between the $2xCO_2$ scenario and the base case scenario, for the 1951-88 period, as resulting from the changed climate.

Transfer of information between the GCMs and GLERL's hydrologic models in the manner described involves several assumptions. Solar insolation at the top of and through the atmosphere on a clear day are assumed to be unchanged under the changed climate, modified only by cloudcover changes. Over-water corrections are made in the same way, albeit with changed meteorology, which presumes that over-water/over-land atmospheric relationships are unchanged. GLERL's procedure for transfering information from the GCM grid to their spatial data is an objective approach but simple in concept. It ignores interdependencies in the various meteorologic variables as all are averaged in the same manner. Of secondary importance, the spatial averaging of meteorologic values over a box centered on the GCM grid point (implicit in the use of the nearest grid point to each square kilometer of interest) filters all variability that exists in the GCM output over that box. If GCM output were interpolated between these point values then at least some of the spatial variability might be preserved. The interpolation performed by Louie from the original GCM grid to a finer grid reduced this problem but it still exists in the use of the finer grid with the hydrology models. Of course, little is known about the validity of various spatial interpolation schemes and, for highly variable spatial data, they may be inappropriate. However, the same is true for the spatial averaging that was used to supply the GCM results for this study.

Steady-state behavior, in all aspects of the hydrological cycle, are exemplified here in figures for the Lake Superior basin and summarized for all lakes and all climate-change scenarios for the entire period in tables.

Basin Meteorology

The annual cycles of all meteorologic variables were averaged over the 1951-88 period and inspected. The $2xCO_2$ climate air temperatures are higher throughout the annual cycle than the $1xCO_2$ climate (base case); the difference is smallest during the late fall to early winter and largest during the late winter to early spring for all lakes; see Fig. 3. The difference is smallest and largest (most variability in the seasonal cycle) for the southern-most lakes. The average annual air temperatures are 4.4-6.1 °C higher, depending on the basin; see Table 3. The $2xCO_2$ climate precipitation is generally higher during the spring and lower during the fall and winter than the $1xCO_2$ climate precipitation over all of the Great Lakes' basins, although generally lower to the south; see Fig. 3. The average steady-state annual

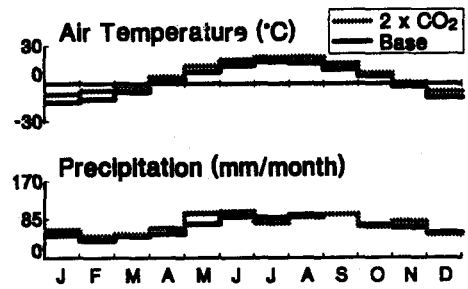

Fig. 3. Steady-State Lake Superior Over-Basin Meteorologic Climate Changes.

precipitation is 8% higher over the Superior basin to 10% lower over the Erie basin with a fairly smooth change with longitude; see Table 3. Precipitation changes and air temperature changes are both fairly consisitent with longitude as illustrated in Table 3.

Basin Hydrology

The resulting average annual steady-state evapotranspiration from the land portion of the basins is higher for the $2xCO_2$ climate in all lake basins, with a fairly smooth change with longitude from 26% higher over the Superior basin to 17% higher over the Erie basin; see Table 3. However, over the seasonal cycle, $2xCO_2$ evapotranspiration exceeds the base case the most in the late spring to early summer (late on Lake Superior basin) and is actually smaller in the early fall, see Fig. 4. Runoff from the land portion of the basin is reduced by the $2xCO_2$ climate in all basins, changing from only 12% lower over the Superior basin to 56% lower over the St. Clair basin in a fairly smooth variation with latitude; see Table 3. The average annual cycle of runoff, depicted in Fig. 4, has changed as well; runoff peaks slightly earlier and with smaller magnitude under the $2xCO_2$ climate than under the $1xCO_2$ climate. This is largely the result of the very big changes observed in the snowpack accumulation and ablation as well as in other basin moisture storages.

On the Superior basin, the average steady-state snowpack storage is reduced by more than half; on the other basins, more to the south, the snowpack is almost entirely absent under the $2xCO_2$ climate; see Fig. 4 and Table 4. This reduction in snowpack accumulation results from the higher air temperatures, especially during the winter, that accompany the changed climate. The snow season is shortened also more than one month. The effects on the snowpack are felt throughout the basin in terms of the derived moisture storages in the soil zone, groundwater, and surface zones. Figure 4 illustrates the general impact of generally lower mois-

Table 3. Average Annual Steady-State Basin Hydrology Differences.

Basin	Air Temperatures and Absolute Differences			Precipitation[a] and Relative Changes		
	$1xCO_2$	$2xCO_2$	Diff.	$1xCO_2$	$2xCO_2$	Diff.
Superior	2.4°	6.8°	4.4°	817 mm	880 mm	8 %
Michigan	7.2°	12.8°	5.6°	825 mm	797 mm	-3 %
Huron	5.4°	10.4°	5.0°	870 mm	852 mm	-2 %
St. Clair	8.3°	14.4°	6.1°	849 mm	772 mm	-9 %
Erie	9.1°	15.1°	6.0°	905 mm	817 mm	-10 %
Ontario	7.2°	12.2°	5.0°	930 mm	879 mm	-6 %
Basin	**Evapotranspiration[a] and Relative Changes**			**Runoff[a] and Relative Changes**		
	$1xCO_2$	$2xCO_2$	Diff.	$1xCO_2$	$2xCO_2$	Diff.
Superior	423 mm	534 mm	26 %	394 mm	346 mm	-12 %
Michigan	507 mm	600 mm	18 %	317 mm	196 mm	-38 %
Huron	493 mm	608 mm	24 %	377 mm	243 mm	-36 %
St. Clair	535 mm	632 mm	18 %	315 mm	140 mm	-56 %
Erie	565 mm	659 mm	17 %	341 mm	158 mm	-54 %
Ontario	472 mm	575 mm	22 %	459 mm	304 mm	-34 %

[a]Expressed as a depth over the land portion of the basin.

Table 4. Average Annual Steady-State Basin Storage Differences.

Basin	Snow Water Equivalent[a] and Relative Changes			Soil Moisture[a] and Relative Changes		
	$1xCO_2$	$2xCO_2$	Diff.	$1xCO_2$	$2xCO_2$	Diff.
Superior	50 mm	24 mm	-51 %	42 mm	36 mm	-14 %
Michigan	12 mm	2 mm	-87 %	35 mm	22 mm	-37 %
Huron	28 mm	6 mm	-79 %	54 mm	40 mm	-26 %
St. Clair	9 mm	1 mm	-91 %	6 mm	2 mm	-67 %
Erie	6 mm	1 mm	-90 %	7 mm	3 mm	-63 %
Ontario	16 mm	2 mm	-85 %	21 mm	14 mm	-31 %
Basin	**Groundwater Moisture[a] and Relative Changes**			**Total Basin Storage[a] and Relative Changes**		
	$1xCO_2$	$2xCO_2$	Diff.	$1xCO_2$	$2xCO_2$	Diff.
Superior	146 mm	124 mm	-15 %	295 mm	237 mm	-20 %
Michigan	61 mm	41 mm	-33 %	114 mm	68 mm	-40 %
Huron	8 mm	5 mm	-39 %	99 mm	57 mm	-43 %
St. Clair	10 mm	5 mm	-51 %	28 mm	9 mm	-67 %
Erie	9 mm	4 mm	-52 %	24 mm	8 mm	-65 %
Ontario	11 mm	7 mm	-36 %	61 mm	33 mm	-46 %

[a]Expressed as a depth over the land portion of the basin.

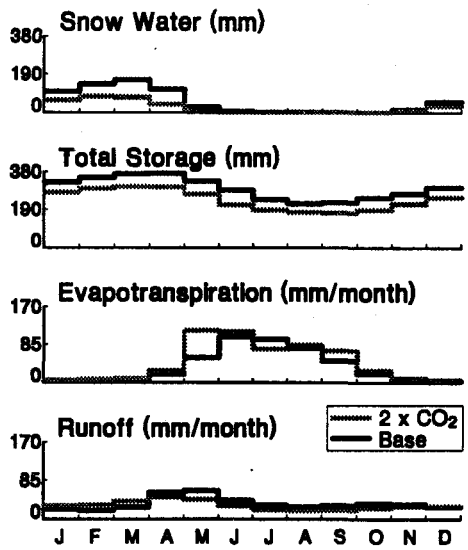

Fig. 4. Steady-State Lake Superior Over-Basin Hydrologic Changes.

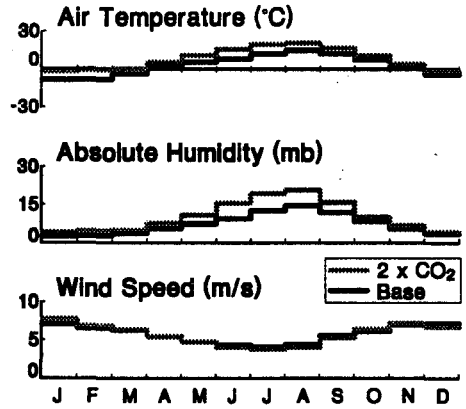

Fig. 5. Steady-State Lake Superior Over-Lake Meteorologic Climate Changes.

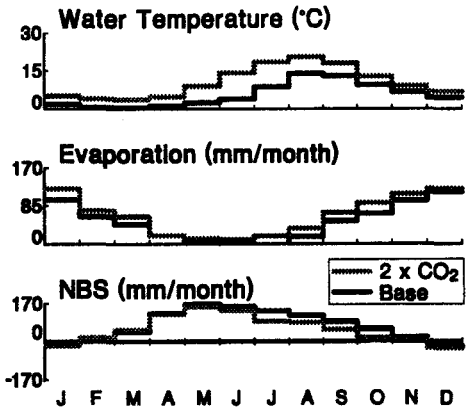

Fig. 6. Steady-State Lake Superior Over-Lake Hydrologic Changes.

ture storages that peak earlier in the $2xCO_2$ climate than in the $1xCO_2$ climate scenarios for all Great Lake basins. This general lowering of moisture in storage in each of the basins is summarized in Table 4 and in some cases represents greater than a 50% reduction in available moisture (see "Total Basin Storage" column).

Over-Water Meteorology

The over-lake air temperature, humidity, and wind speed differs from over-land since the lower atmospheric layer is affected by the water surface over which it lies. The model corrections to over-land meteorology observations for over-water conditions depend heavily on the water surface temperature which in turn is a function of the over-lake meteorology and heat balance at the surface of the lake. Figure 5 illustrates the $2xCO_2$ and the base case annual cycles for Superior over-lake meteorology (air temperature, absolute humidity, and wind speed), and Fig. 6 illustrates water temperature, evaporation, and net basin supply. In general, the synergistic relationship that exists between air and water temperature in the $2xCO_2$ scenario yields a general increase in both that follows the $1xCO_2$ climate patterns, similar to over-land behavior in Figs. 5 and 6. The most pronounced increase in both occurs in the summer for Lake Superior. Table 5 shows that the average steady-state air temperature difference between the $2xCO_2$ and base cases varies from 5.3 °C on Lakes Superior and Huron to 5.9 °C on Lake Michigan. Variations in the impact with latitude or longitude or size of the lake are not pronounced, in terms of volume or heat capacity. Relative humidity over the lakes is increased, probably due to the increased lake evaporation, and cloud cover generally has decreased slightly for the $2xCO_2$ climate; see Fig. 5 and Table 5. Again, the difference is most pronounced in the summer. Over-water wind speed is not greatly affected after correction of over-land values for over-water conditions at increased water temperatures; Fig. 5 and Table 5 show only a slight decrease for each lake in

Table 5. Average Annual Steady-State Over-Lake Meteorology Differences.

Basin	Air Temperatures and Absolute Differences			Absolute Humidity and Absolute Differences		
	$1xCO_2$	$2xCO_2$	Diff.	$1xCO_2$	$2xCO_2$	Diff.
Superior	3.1°	8.4°	5.3°	7.2 mb	10.3 mb	3.1 mb
Michigan	7.7°	13.6°	5.9°	9.7 mb	13.3 mb	3.6 mb
Huron	6.5°	11.8°	5.3°	9.0 mb	12.4 mb	3.4 mb
St. Clair	10.3°	16.0°	5.7°	11.2 mb	15.1 mb	3.9 mb
Erie	9.7°	15.3°	5.6°	10.9 mb	14.7 mb	3.8 mb
Ontario	8.0°	13.4°	5.4°	9.8 mb	13.6 mb	3.8 mb
Basin	**Cloud Cover and Relative Changes**			**Wind Speed and Relative Changes**		
	$1xCO_2$	$2xCO_2$	Diff.	$1xCO_2$	$2xCO_2$	Diff.
Superior	0.57	0.58	2 %	5.7 m/s	5.7 m/s	0 %
Michigan	0.43	0.42	-2 %	6.1 m/s	5.9 m/s	-3 %
Huron	0.55	0.55	-1 %	6.0 m/s	5.9 m/s	-2 %
St. Clair	0.50	0.47	-4 %	5.7 m/s	5.6 m/s	-2 %
Erie	0.63	0.61	-3 %	6.3 m/s	6.1 m/s	-3 %
Ontario	0.59	0.58	-1 %	6.1 m/s	6.0 m/s	-2 %

Table 6. Selected Average Annual Steady-State Hydrology Differences.

Basin	Water Temperature and Absolute Differences			Over-Lake Evaporation[a] and Relative Changes		
	$1xCO_2$	$2xCO_2$	Diff.	$1xCO_2$	$2xCO_2$	Diff.
Superior	5.4°	10.5°	5.1°	561 mm	736 mm	31 %
Michigan	8.5°	14.1°	5.6°	647 mm	854 mm	32 %
Huron	8.0°	13.0°	5.0°	627 mm	829 mm	32 %
St. Clair	1.0°	15.8°	4.8°	936 mm	1234 mm	32 %
Erie	10.9°	15.8°	4.9°	898 mm	1197 mm	33 %
Ontario	9.0°	14.4°	5.4°	665 mm	874 mm	31 %

[a]Expressed as depths over the lake.

steady-state windspeed averages.

Lake Heat Balance

The heat budget gives rise to increased water surface temperatures as seen in Fig. 6 and summarized in Table 6. The average steady-state increase in water surface temperatures for the $2xCO_2$ scenario range from 4.8 °C on Lake St. Clair to 5.6 °C on Lake Michigan. The heat storage capacity of a lake has an influence on the increase in water surface temperatures that can almost be seen in Fig. 6. Water surface temperatures are seen to peak earlier on deep lakes under the $2xCO_2$ climate than under the $1xCO_2$ climate. Large amounts of heat now reside in the deep lakes throughout the year, increasing latent and sensible transfers to the atmosphere; see Fig. 6. The increased heat in storage also means that ice formation will be greatly reduced over winter on the deep Great Lakes. The higher water surface temperatures under the $2xCO_2$ climate result in increased annual lake evaporation of about 31-33%; see Table 6. The increased heat storage also changes temperature-depth profiles in the lakes.

Some of the deep lakes (Michigan, Huron, and Ontario) show water surface temperatures that stay above 3.98 °C throughout the average annual cycle. Figure 7 illustrates this for 1961 on Lake Superior.

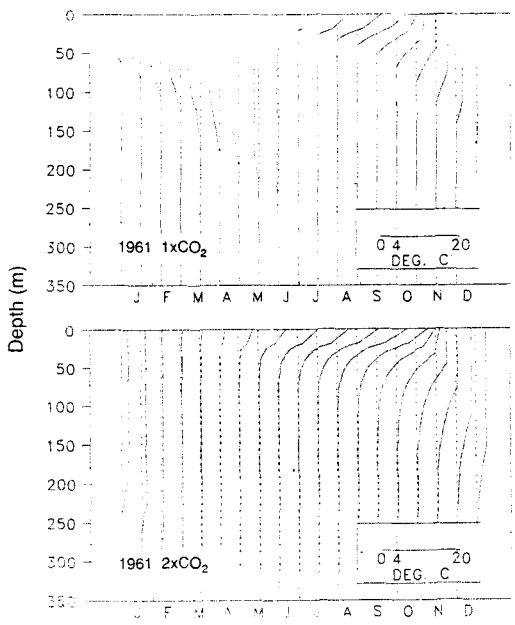

Fig. 7. Steady-State Lake Superior Temperature-Depth Profiles.

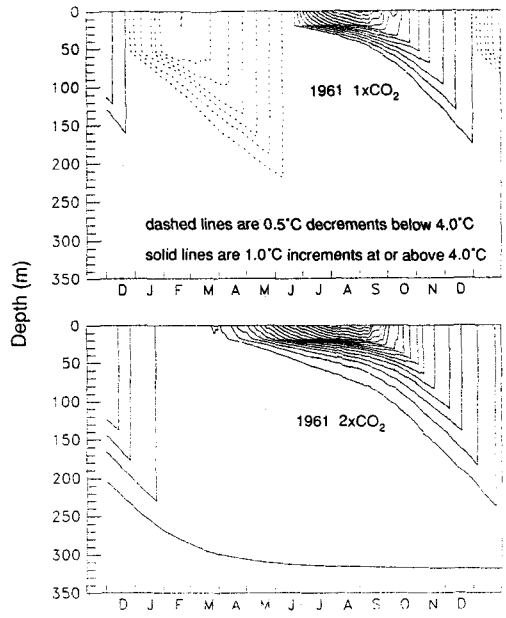

Fig. 8. Steady-State Lake Superior Depth-Time Temperature Isolines.

This means that bouyancy-driven turnovers of the water column do not occur in the same way as they do at present.

In some years, the large lakes are changed from dimictic lakes (turnovers occur twice a year as water temperatures pass through the point of maximum density, 3.98 °C) to monomictic lakes (maximum turnover occurs at the temperature "reversal" where temperatures stop declining and start rising again and the minimum temperature is greater than 3.98 °C). Figure 7 shows that the $1xCO_2$ temperature profile for Lake Superior passed through 3.98°C in June 1961 and approached, in December, the January 1962 transition. Under the $2xCO_2$ scenario, temperatures remain above 3.98°C but approach a vertical profile most in March. This represents a change from dimictic to monomictic.

Table 7 shows that the large lakes remain dimictic under the $2xCO_2$ climate only between 2% and 76% of the time. The largest change is associated with Lake Ontario which is the furthest south of the deep lakes. Least effected are Lakes Erie and St.Clair which are very shallow and have relatively little heat storage. As the lakes move to one reversal per year in some years, instead of two turnovers per year, the interarrival times of the maximum mixing extent increase. Table 7 illustrates that the average interarrival time grows to nearly a full year on Lake Ontario since only 2% of the years have dimictic behavior. Table 7 also illustrates the monomictic reversal temperature is, of course, well above the point of maximum water density.

The timing, of maximum turnovers or temperature reversals, shifts. Table 8 shows the time between the spring turnover and the fall turnover (for dimictic behavior) increases. The spring turnover occurs earlier and the fall turnover occurs later in the annual cycle. For monomictic behavior, the single maximum turnover occurs even earlier in the year than the dimictic turnovers. These are consequences of greater heat storage in, and heat inputs to, the lakes.

Temperature-depth profiles for every day of a single model year can be combined and depicted as depth-time plots of temperature isolines; see Fig. 8 for an example on Lake Superior. Then, not only are the turnover timing changes depicted between $1xCO_2$ and $2xCO_2$ climates, but depth changes are more apparent as well. Table 8 also summarizes the maximum depths at turnover in the lakes. Dimicitic spring turnovers exhibit shallower average depths under $2xCO_2$ condi-

Table 7. Average Characteristics of Turnovers/Reversals.

	Fraction Dimictic		Interarrival Times		$2xCO_2$ Monomictic Reversal
	$1xCO_2$	$2xCO_2$	$1xCO_2$	$2xCO_2$	Water Temperature
Superior	100 %	67 %	182 d	211 d	4.5 °C
Michigan	100 %	15 %	182 d	318 d	4.9 °C
Huron	100 %	24 %	182 d	292 d	4.9 °C
St. Clair	100 %	100 %	183 d	185 d	
Erie	100 %	76 %	183 d	206 d	4.9 °C
Ontario	100 %	2 %	182 d	356 d	5.9 °C

Table 8. Average Dates and Depths of Maximum Turnover or Temperature Reversal.

Basin	$1xCO_2$		$2xCO_2$		
	Dimictic		Dimictic		Monomictic
	Spring	Fall	Spring	Fall	
			DATES		
Superior	02 Jul	23 Dec	24 Apr	11 Feb	24 Mar
Michigan	27 May	01 Jan	27 Mar	28 Jan	22 Feb
Huron	26 May	10 Jan	26 Mar	11 Feb	10 Mar
St. Clair	30 Apr	20 Nov	04 Mar	28 Nov	
Erie	30 Apr	24 Dec	03 Mar	06 Jan	01 Feb
Ontario	20 May	18 Jan	10 Mar	29 Jan	03 Mar
			DEPTHS		
Superior	234 m	162 m	127 m	257 m	297 m
Michigan	132 m	111 m	52 m	199 m	231 m
Huron	229 m[a]	229 m[a]	140 m	229 m[a]	229 m[a]
St. Clair	6 m[a]	6 m[a]	6 m[a]	6 m[a]	
Erie	64 m[a]	64 m[a]	48 m	64 m[a]	53 m
Ontario	232 m	242 m	70 m	244 m[a]	244 m[a]

[a]Maximum average depth of the lake.

tions and fall turnovers are deeper, where not limited by the depth of the lake. Monomictic turnovers are generally even deeper.

There is a normal hysteresis observed in graphs of lake heat plotted with surface temperature, such as in Fig. 9. This reflects the mixing of heat at depth. Surface temperatures rise quickly, and heat storage follows after the spring turnover. When surface temperatures then begin to drop in the fall, stored heat initially does not. Then heat storage drops more slowly. Similar behavior occurs after the fall turnover, and both result in the characteristic double "loop" in the plot. Under the warmer climate change scenario, temperatures sometimes never drop below that at maximum density (3.98°C). This results in only one hysteresis loop, but it is much larger.

Net Supply Components

Over-lake precipitation, runoff, and lake evaporation sum algebraically as the net basin supply and are presented again in Table 9 for convenience. Since over-lake precipitation is taken here as the same as overland, Table 9 shows the same relations for $2xCO_2$ vs. base case precipitation as does Table 4. Net basin supply in Table 9 is seen to be less under the $2xCO_2$ climate than under the $1xCO_2$ climate on all lakes. This is true throughout the year for Lake Erie and nearly true on the other lakes (see Fig. 6). Net basin supplies are lower throughout the annual cycle except for February and March on Lake Superior, February on Lakes

Table 9. Average Annual Steady-State Net Supply Components Differences.

Basin	Over-Lake Precipitation[a] and Absolute Differences			Basin Runoff[a] and Absolute Differences		
	$1xCO_2$	$2xCO_2$	Diff.	$1xCO_2$	$2xCO_2$	Diff.
Superior	817 mm	880 mm	63 mm	615 mm	539 mm	-75 mm
Michigan	825 mm	797 mm	-28 mm	635 mm	393 mm	-242 mm
Huron	869 mm	852 mm	-18 mm	836 mm	539 mm	-297 mm
St. Clair	849 mm	772 mm	-77 mm	4453 mm	1980 mm	-2474 mm
Erie	905 mm	817 mm	-88 mm	803 mm	372 mm	-431 mm
Ontario	930 mm	879 mm	-51 mm	1694 mm	1123 mm	-571 mm

Basin	Over-Lake Evaporation[a] and Absolute Differences			Net Basin Supply[a] and Relative Changes		
	$1xCO_2$	$2xCO_2$	Diff.	$1xCO_2$	$2xCO_2$	Diff.
Superior	561 mm	736 mm	175 mm	871 mm	684 mm	-21 %
Michigan	647 mm	854 mm	207 mm	813 mm	336 mm	-59 %
Huron	627 mm	829 mm	202 mm	1079 mm	562 mm	-48 %
St. Clair	936 mm	1234 mm	298 mm	4367 mm	1517 mm	-65 %
Erie	898 mm	1197 mm	299 mm	810 mm	-8 mm	-101 %
Ontario	665 mm	874 mm	209 mm	1959 mm	1127 mm	-42 %

[a]Expressed as depths over the lake.

Table 10. Average Annual Steady-State Great Lakes Basin Hydrology and Net Basin Supply Components.

Scen-ario	Over Land Precip-itation	Evapo-trans-piration	Basin Runoff	Over Lake Precip-itation	Over Lake Evap-oration	Net Basin Supply
	(cms)	(cms)	(cms)	(cms)	(cms)	(cms)
$1xCO_2$	13815	7825	5987	6604	4992	7783
$2xCO_2$[a]	13598	9518	4077	6578	6587	4180
CCC[a]	-2%	22%	-32%	0%	32%	-46%
GISS[b]	2%	21%	-24%	4%	27%	-37%
GFDL[c]	1%	19%	-23%	0%	44%	-51%
OSU[d]	6%	19%	-11%	6%	26%	-23%

[a]Canadian Climate Centre, prepared by Louie (1991).
[b]Goddard Institute for Space Studies GCM, used by Croley (1990).
[c]Geophysical Fluid Dynamics Laboratory GCM, used by Croley (1990).
[d]Oregon State University GCM, used by Croley (1990).

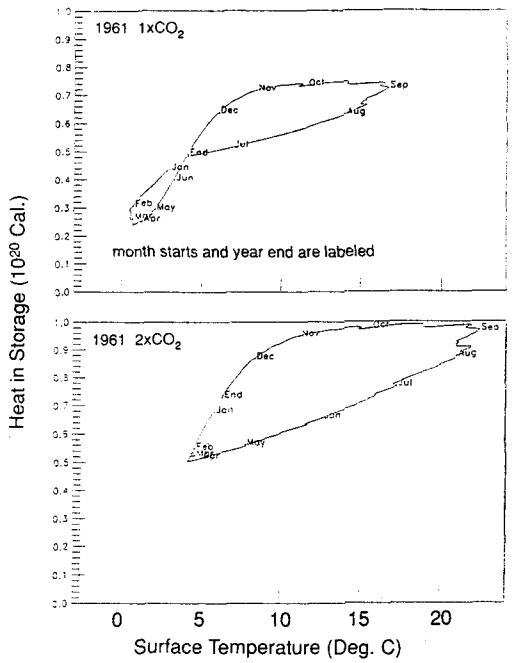

Fig. 9. Steady-State Lake Superior Heat-Temperature Hysteresis.

Michigan and Huron, January on Lake St. Clair, and January and February on Lake Ontario. Table 10 summarizes the changes in the hydrologic and net basin supply components for the entire Great Lakes basin; they were computed by converting the equivalent depths of Table 9 to annual flow rates on each lake and adding them over all the lakes. The changes from the base case are also expressed relatively in Table 10. Also expressed relatively are changes from other studies that used other general circulation models (Croley, 1990); they are provided for comparison. Net basin supplies to all Great Lakes are seen to drop to about one half under the CCC GCM; this corresponds to the GCM from the Geophysical Fluid Dynamics Laboratory (GFDL) in the earlier studies. This drop in net basin supply seems to result from the increases in lake evaporation and overland evapotranspiration (reducing subsequent runoff to the lakes) observed in the $2xCO_2$ scenario from the GCM.

Sensitivities

Without temperatures below freezing, the snowpack is insensitive to precipitation. Although the steady-state scenarios on different lakes show different estimates of precipitation change, each shows increases in air temperatures that significantly reduce the snowpack, especially in the southern basins. Thus, even if precipitation increases more than suggested by the GCM, the snowpack will be much reduced under warmer winters. Similarly, regardless of actual changes in precipitation, the Great Lakes basin will experience reduced soil moisture storage and runoff. Both peak shortly after snowmelt, and then drop throughout the summer and fall, due to high evapotranspiration; each climate scenario produces earlier snowmelt and a longer period of evapotranspiration. Although soil moisture and runoff certainly vary with precipitation, they are most sensitive to it in midsummer when at their annual minimums. Thus, within the limits of precipitation produced by the GCMs, soil moisture and runoff scenarios are relatively insensitive to precipitation.

Of the meteorological variables that affect lake evaporation (air temperature, humidity, cloud cover, and wind speed) wind speed is probably the most critical, although air temperature and humidity are also important. Across all lakes and scenarios, daily evaporation was reduced (compared to the base case) only when the scenarios showed reduced wind speeds. If wind speeds remain near historical levels, evaporation will still increase somewhat, however, due simply to the increase in air temperatures that then increase water temperatures. Thus, within the range of other meteorologic variables shown by the GCMs, only if wind speeds are less than historical levels by about 0.5% will lake evaporation not increase.

Because net basin supplies are a sum of lake evaporation, runoff, and precipitation, they are equally sensitive to changes in any of the components. Thus, as long as wind speeds are not much less than historical levels, regardless of precipitation changes (unless much larger than any shown by the GCMs), net basin supplies are likely to drop due to higher air temperatures that increase evaporation and decrease runoff.

Summary

The study results should be received with caution as they are of course dependent on the GCM outputs, which have large uncertainties. The linkage method used here does not recognize interdependencies between meteorological variables. It also simply changes the magnitude of meteorological time series without affecting their temporal structures. Therefore, changes in variabilities that would take place under a changed climate are not addressed. Seasonal timing differences in the GCM for the changed climate are not reproduced with this method of coupling. Instead, while seasonal meteorology patterns are preserved in the $2xCO_2$ scenario as they exist in the $1xCO_2$ historical data, one still can observe seasonal changes induced by storage

effects. Water temperatures increase and peak earlier; heat resident in the deep lakes increases throughout the year. Mixing of the water column diminishes, as most of the lakes become mostly monomictic, and lake evaporation increases. Changes in annual variability are less clear, again as a result of using the same historical time structure for both the base case and the changed climate scenarios.

The higher air temperatures under the $2xCO_2$ scenarios lead to higher over-land evapotranspiration and lower runoff to the lakes with earlier runoff peaks since snowpack is reduced up to 100% and the snow season is shortened more than one month. This also results in a reduction in available soil moisture. Water surface temperatures peak earlier and are higher with larger amounts of heat resident in the deep lakes throughout the year. Also, bouyancy-driven turnovers of the water column do not occur as often on all lakes except St. Clair. Currently, they occur twice a year on all lakes. Without biannual turnovers, hypolimnion chemistry may be altered; oxygen may be depleted, releasing nutrients and metals from lake sediments. The lakes may experience more than a single winter turnover if temperature gradients are small and winds are strong enough to induce turbulent mixing (Hutchinson, 1957). Ice formation will be greatly reduced over winter on the deep Great Lakes, and lake evaporation will increase. The average steady-state net supplies to all lakes are seen to drop.

REFERENCES

Assel, R.A. 1983. *NOAA Data Report ERL GLERL-24*, Great Lakes Environmental Research Laboratory, Ann Arbor

Blumberg, A.F. & DiToro, D.M. 1989. In Smith, J.B. & Tirpak, D.A. (Eds.) *The Potential Effects of Global Climate Change on the United States, Appendix A: Water Resources*, EPA-230-05-89-051, U. S. Environmental Protection Agency, Washington, pp 7-1 - 7-28.

Bolsenga, S.J. 1977. *J. Appl. Meteorol.*, **16**(11):1158-1164

Bolsenga, S.J. 1979. *J. Great Lakes Res.*, **5**(3-4):301-311

Bolsenga, S.J. & Hagman, J.C. 1975. In *Int. Field Year for the Great Lakes Bull. 16*, National Oceanic and Atmospheric Administration, Rockville, pp 57-62.

Cohen, S.J. 1991. In *Proceedings of A Symposium on Climate Scenarios*, The Water Network, University of Waterloo, Waterloo, pp 16-32.

Croley, T.E., II 1982. *NOAA Tech. Memo. ERL GLERL-39*, National Technical Information Service, Springfield

Croley, T.E., II 1983a. *J. Hydrol.*, **64**:135-158

Croley, T.E., II 1983b. *J. Hydrol.*, **66**:101-121

Croley, T.E., II 1989a. *NOAA Tech. Memo. ERL GLERL-70*, Great Lakes Environmental Research Laboratory, Ann Arbor

Croley, T.E., II 1989b. *Wat. Resour. Res.*, **25**(5):781-792

Croley, T.E., II 1990. *Clim. Change*, **17**:27-47

Croley, T.E., II 1991. In *Proceedings of A Symposium on Climate Scenarios*, The Water Network, University of Waterloo, Waterloo, pp 33-48.

Croley, T.E., II 1992a. *Wat. Resour. Res.*, **28**(1):69-81

Croley, T.E., II 1992b. In *Proceedings of the Symposium on Managing Water Resources During Global Change*, Twenty-Eighth American Water Resources Association Conference, pp 241-250.

Croley, T.E., II 1993a. In *Climate, Climate Change, Water Level Forecasting and Frequency Analysis, Supporting Documents, Volume 1 - Water Supply Scenarios*, International Joint Commission, Washington, pp 9-1 - 9-33.

Croley, T.E., II 1993b. *Wat. Resour. Bull.*, **29**(5)

Croley, T.E., II & Assel, R.A. 1993. *Wat. Resour. Res.*, (in press)

Croley, T.E., II & Hartmann, H.C. 1984. *NOAA Tech. Memo. ERL GLERL-50*, National Technical Information Service, Springfield

Croley, T.E., II & Hartmann, H.C. 1985. *J. Hydrol.*, **76**:363-379

Croley, T.E., II & Hartmann, H.C. 1986. *NOAA Tech. Memo. ERL GLERL-61*, Environmental Research Laboratories, Boulder

Croley, T.E., II & Hartmann, H.C. 1987. *J. Wat. Resour. Plan. Manag. Div.* (Amer. Soc. Civil Eng.), **113**(6):810-823

Croley, T.E., II & Hartmann, H.C. 1989. In Smith, J.B. & Tirpak, D.A. (Eds.) *The Potential Effects of Global Climate Change on the United States, Appendix A: Water Resources*, EPA-230-05-89-051, U. S. Environmental Protection Agency, Washington, pp 4-1 - 4-34.

Croley, T.E., II & Lee, D.H. 1993. *Wat. Resour. Bull.*, **29**(2):267-282

Gauthier, R.L., Melloh, R.A., Croley, T.E., II & Hart-

mann, H.C. 1984. In *Proceedings 18th International Symposium on Remote Sensing of the Environment*, Paris, pp 1-12.

Gray, D.M., McKay, G.A. & Wigham, J.M. 1973. In Gray, D.M. (Ed.) *Handbook on the Principles of Hydrology*, Water Information Center, New York, pp 3.1-3.66.

Green, G.M. & Outcalt, S.I. 1985. *Cold Reg. Sci. & Technol.*, **10**:251-262

Hartmann, H.C. 1987. *NOAA Tech. Memo. ERL GLERL-66*, Great Lakes Environmental Research Laboratory, Ann Arbor

Hartmann, H.C. 1988. *J. Great Lakés Res.*, **14**(3):316-324

Hartmann, H.C. 1990. *Clim. Change*, **17**:49-67

Hostetler, S.W. & Bartlein, P.J. 1990. *Wat. Resour. Res.*, **26**(10):2603-2612

Hutchinson, G.E. 1957. *A Treatise on Limnology, Volume I, Part 1 - Geography and Physics of Lakes*, John Wiley and Sons, New York

International Great Lakes Diversions and Consumptives Uses Study Board, 1981. *Great Lakes Diversions and Consumptive Uses*. International Joint Commission, Washington

International Lake Superior Board of Control, 1981. *Regulation of Lake Superior: Plan 1977 Development, Description, and Testing*. International Joint Commission, Washington

International Lake Superior Board of Control, 1982. *Regulation of Lake Superior: Operational Guides for Plan 1977*. International Joint Commission, Washington

International St. Lawrence River Board of Control, 1963. *Regulation of Lake Ontario: Plan 1958-D*. International Joint Commission, Washington

Keijman, J.Q. 1974. *Bound.-Layer Meteor.* **7**:399-407

Kraus, E.B. & Turner, J.S. 1967. *Tellus* **19**:98-105

Louie, P.Y.T. 1991. In *Proceedings of A Symposium on Climate Scenarios*, The Water Network, University of Waterloo, Waterloo, pp 67-78.

McCormick, M.J. & Meadows, G.A. 1988. *J. Geophys. Res.*, **93**(C6):6774-6788

McCormick, M.J. 1989. In Smith, J.B. & Tirpak, D.A. (Eds.) *The Potential Effects of Global Climate Change on the United States, Appendix A: Water Resources*, EPA-230-05-89-051, U. S. Environmental Protection Agency, Washington, pp 6-1 - 6-26.

McFarlane, N.A. 1991. In *Proceedings of A Symposium on Climate Scenarios*, The Water Network, University of Waterloo, Waterloo, pp. 3-15.

McFarlane, N.A., Boer, G.J., Blanchet, J.P. & Lazare, M. 1991. *J. Climatol.*, (in press)

Phillips, W.D. & Irbe, J.G. 1978. *Report CLI-2-77*, Environment Canada, Atmospheric Environment Service, Downsview

Quinn, F.H. 1978. *J. Hydrol.*, **37**:295-307

Quinn, F.H. 1979. *Wat. Resour. Res.*, **15**(4):935-940

Wilson, J.W. 1977. *Month. Weath. Rev.* **105**:207-214